Article

Influence of surface properties of filtration-layer metal oxide on ceramic membrane fouling during ultrafiltration of oil/water emulsion

Dongwei Lu, Tao Zhang, Leo Gutierrez, Jun Ma, and Jean-Philippe Croue

Environ. Sci. Technol., **Just Accepted Manuscript** • DOI: 10.1021/acs.est.5b04151 • Publication Date (Web): 01 Apr 2016

Influence of surface properties of filtration-layer metal oxide on ceramic membrane fouling during ultrafiltration of oil/water emulsion

Submitted by

Dongwei Lu [a], Tao Zhang [b], Leo Gutierrez [c,d], Jun Ma [a] and Jean-Philippe Croué [b,c**]*

a. State Key Laboratory of Urban Water Resource and Environment, Harbin Institute of Technology, Harbin 150090, People's Republic of China

b. Water Desalination and Reuse Center, King Abdullah University of Science and Technology, Thuwal 4700, Kingdom of Saudi Arabia

c. Curtin Water Quality Research Centre, Department of Chemistry, Curtin University of Technology, Australia

d. Facultad del Mar y Medio Ambiente, Universidad del Pacifico, Guayaquil, Ecuador

TOC Art

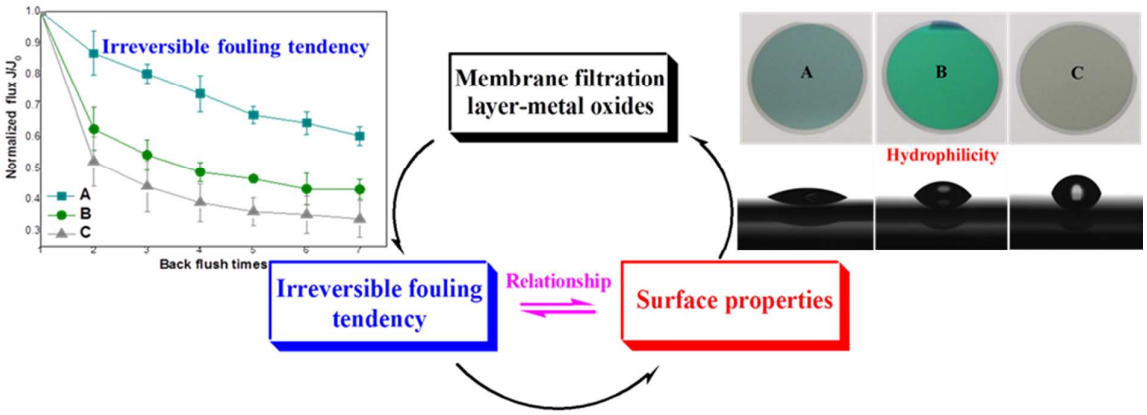
Irreversible fouling tendency
Normalized flux J/J0
Back flush times
A
B
C
Membrane filtration layer-metal oxides
Hydrophilicity
Irreversible fouling tendency
Relationship
Surface properties

ABSTRACT

In this work, ceramic ultrafiltration membranes deposited with different metal oxides (i.e., TiO_2, Fe_2O_3, MnO_2, CuO, and CeO_2) of around 10 nm in thickness and similar roughness were tested for O/W emulsion treatment. Distinct membrane fouling tendency was observed, which closely correlated to the properties of the filtration-layer metal oxides (i.e. surface hydroxyl groups, hydrophilicity, surface charge, and adhesion energy for oil droplets). In consistent with the distinct bond strength of the surface hydroxyl groups, hydrophilicity of these common metal oxides are quite different. The differences in hydrophilicity consequently lead to different adhesion of these metal oxides towards oil droplets which consists very well with irreversible membrane fouling tendency. In addition, the surface charge of the metal oxide opposite to that of emulsion can help to alleviate irreversible membrane fouling in ultrafiltration. Highly hydrophilic Fe_2O_3 with lowest fouling tendency could be a potential filtration-layer material for the fabrication/modification of ceramic membranes for O/W emulsion treatment. To the best of our knowledge, this is the first study clearly showing the correlations between surface properties of filtration-layer metal oxides and ceramic membrane fouling tendency by O/W emulsion.

INTRODUCTION

Oily wastewater is produced in large volumes by many industries (e.g., oil and gas extraction, petroleum refining, food industry, and metal manufacturing).[1, 2] The oil in water is commonly classified as free oil (Dp > 100 um), dispersed oil ((Dp = 100-10 um), emulsified oil (Dp < 10 μm), and dissolved oil, among which O/W emulsion and dissolved oil compounds are most difficult to be effectively removed. Oil-in-water (O/W) emulsions are usually stabilized by emulsifier (e.g., surfactant) which reduces the interfacial tension between oil and water.[3] Most of environmental guidelines require that the maximum oil and grease concentrations in effluents should be less than 10-15 mg/L (in some countries < 5 mg/L), making efficient removal of O/W emulsion very critical in the treatment of oily wastewater.[4] Most of the conventional processes for O/W emulsion treatment (e.g., gravity separation, chemical demulsification, air flotation, etc.), are not efficient enough in the treatment of stable O/W emulsions to meet the standards.[5-7] These processes also have disadvantage such as significant recontamination and high operation cost.[8-10]

Ultrafiltration (UF) has been widely studied for O/W emulsion treatment to replace traditional treatment because of its relatively low operation cost, steady quality of permeate, and small space requirement.[11-13] Ceramic membranes are considered to be superior to polymeric membranes for the treatment of oily wastewater as they have higher mechanical, chemical, and thermal stability, as well as possibly overall lower lifecycle cost.[14-16] However, like polymeric membranes, ceramic membranes also suffer from fouling during the treatment of O/W emulsions.[17] Membrane fouling

(including reversible and irreversible fouling) leads to severe decline of permeate flux and thus compromises the membrane performance. During the filtration of oily wastewater, reversible fouling caused mainly by the accumulation and deposition of oil foulants on membrane surface can be effectively reduced by hydraulic washing (e.g., cross flow and back flush).[17, 11, 18, 19] In contrast, irreversible fouling cannot be effectively reduced merely by hydraulic washing, which therefore is one of the major challenges to ceramic UF membrane in O/W emulsion treatment. The irreversible fouling can be ascribed to: 1) blockage of oil droplets inside membrane pores, and 2) strong adsorption of oil foulant on membrane surface and pores.[20] The first reason of irreversible-fouling is mainly related to the structure and pore size of the membrane as well as the size of oil droplets.[21] The second one is largely determined by the interaction between membrane filtration-layer material and oil foulant.[22, 23] For O/W emulsion treatment, strong oil adsorption could be the main reason causing irreversible fouling due to oil foulant properties such as high viscosity. In such circumstance, ceramic membrane filtration-layer material will play an important rule for the irreversible fouling.

Polymeric membrane materials have been investigated intensively for their antifouling performances during oily wastewater treatment, and the influences of material properties have been widely reported.[22-24] In contrast, roles of ceramic membrane materials in their antifouling performances have not been systematically studied.[25, 26] Knowledge on relationships between surface properties of filtration-layer metal oxide and ceramic membrane fouling tendency will be critical to select

appropriate materials for fabrication/modification of ceramic membrane to successfully treat O/W emulsion.

In this research, five common metal oxides (i.e. TiO_2, Fe_2O_3, MnO_2, CuO, and CeO_2) were selected for experiment due to their high stability in water and relatively low prices. These metal oxides are also widely used as supports for catalysts,[27, 28] thus enabling future fabrication of catalytic membranes to mitigate membrane fouling for the treatment of O/W emulsions.[18, 29, 30] These metal oxides were deposited separately on commercial ceramic membranes (the filtration layer is composed of ZrO_2) with pulsed laser deposition (PLD) to achieve very thin deposition layers (around 10 nm) while without changing membrane roughness and permeability. The irreversible fouling on the deposited membranes was investigated through the treatment of crude oil/water emulsion. Surface properties of these metal oxides were comprehensively characterized in terms of surface hydroxyl groups, hydrophilicity, surface charge, and adhesion energy for oil droplets. The irreversible membrane fouling tendency was correlated to these surface properties of filtration-layer metal oxide. The relationships between surface properties of the filtration layer and the membrane fouling tendency in the treatment of O/W emulsion was, for the first time, clearly demonstrated for ceramic membrane, which can provide a basic knowledge to select/prepare/modify ceramic membranes for sustainable O/W emulsion treatment.

EXPERIMENTAL SECTION

Preparation and characterization of O/W emulsion

Crude oil (provided by Saudi Aramco) was used as base oil to prepare oil/water (O/W) emulsions. Sodium dodecyl benzene sulfonate (SDBS) (Sigma-Aldrich) was used as surfactant to disperse and stabilize the crude oil droplets in preparation of O/W emulsions. Details of the emulsion preparation procedure were provided in **Text S1** of the Supporting Information (**SI**).

The O/W emulsion was characterized in terms of oil-droplet size distribution and zeta potential which were analyzed with a particle size and zeta potential analyzer (Nano ZS, Malvern). Microscopic configuration of the oil droplets was characterized with confocal laser scanning microscopy (CLSM) (LSM710, Carl Zeiss) using Nile red (Sigma-Aldrich) as a stain.[31]

The emulsion has an average oil droplet size of 360 nm after 50 min sonication **(Table S1 and Figure S1, SI)**. It was negatively charged with zeta potentials approaching -45.5 mV at pH 6.0. **Figure S2 (SI)** shows that the fine oil droplets distributed uniformly in the emulsion solution. During the experiments, the as-prepared emulsion was relatively stable in droplet size distribution and zeta potential**.**

Ultrafiltration of O/W emulsion with ceramic membranes

TiO_2, MnO_2, Fe_2O_3, CuO, and CeO_2 (Sigma-Aldrich) were deposited separately onto the filtration layer (composed of ZrO_2) of commercial ceramic membranes (50 kDa, TAMI Industries) by Pulsed-Laser Deposition (PLD) (COMPexPro201, Coherent) technique under specific conditions (**Text S2，SI**) with nearly the same coating thickness (around 10 nm). The coating of five metal oxides on membrane surface was

146 further tested by scanning transmission electron microscopy (STEM) (Titan 80-300,
147 FEI) (**Figure S3**, **SI)**. The elements of the coated metal oxide were confirmed with the
148 Energy Dispersive Spectroscopy (EDS) accessory of the STEM equipment (**Figure**
149 **S4**, **SI**). Morphologies of the virgin membrane and metal oxide-deposited membranes
150 were characterized with scanning electron microscopy (SEM) (Magellan 400, FEI) and
151 Atomic Force Microscopy (AFM) (Agilent 5500, Agilent). The surface roughness and
152 zeta potential of these membranes were measured by AFM and Electrokinetic
153 Analyzer for Solid Samples (SurPASS, Anton Paar), respectively. Details of the
154 filtration procedure were provided in **Text S3 (SI)**. Irreversible fouling of the
155 membranes were evaluated with normalized initial permeate flux of each filtration
156 cycle (NIF_n) which denotes the recovery extent of the permeability by hydraulic back
157 flush. The higher NIF is, the less irreversible fouling the membrane has.
158 The normalized initial permeate flux of each cycle (NIF_n) was calculated with
159 equation (1).

160 $$NIF_n = J_n / J_0 \times 100\% \quad (1)$$

161 J_n denotes the initial permeate flux after each back flush; J_0 is pure water permeate
162 flux of the virgin membrane.
163 Instantaneous permeate flux J (L m^{-2} h^{-1}) was calculated with equation (2).

164 $$J = V/A\Delta t \quad (2)$$

165 V (L) is the permeate volume; A (m^2) denotes the membrane filtration area; and Δt (h)
166 represents filtration duration.
167 Chemical oxygen demand (COD) of the feed and the permeate was measured in
168 triplicate with a COD analyzer (DR2000, Hach). The COD rejection rate (R %) was

calculated with equation (3).

$$R = (1-C_p/C_f) \times 100\% \quad (3)$$

R is the COD removal rate; C_f and C_p are COD concentrations of the feed and the permeate, respectively.

Characterization of surface properties of metal oxide

The surface properties of five metal oxides were investigated in terms of surface hydroxyl groups, hydrophilicity, surface charge, and adhesion energy for oil droplets. The surface hydroxyl groups were examined with Fourier Transform Infrared Spectroscopy (FTIR) equipped with an Attenuated Total Reflection module (ATR) (Nicolet 6700-continuum FT-IR Microscope, Thermo Scientific) with a procedure described in **Text S4 (SI)**. Isoelectric points of metal oxides were measured with a Zeta potential analyzer (Nano ZS, Malvern) as detailed in **Text S5 (SI)**. The hydrophilicity of metal oxide was characterized with contact angle measurement (Attension, KSV). Since the contact angle is influenced by surface roughness of the solid sample,[32, 33] the metal oxides were deposited on smooth silicon wafers (roughness < 0.5 nm) separately with PLD to minimize the roughness effect.[34, 35] The roughness of the deposited wafers was measured with Atomic Force Microscopy (AFM) (Agilent 5500, Agilent) to be below 10 nm (**Table S2, SI**). Contact angle of each deposited metal–oxide layer on the wafer was measured 10 times using a water-droplet volume of 5 ± 0.2 μL. Mean value of the contact angles was calculated, and the standard deviation was below 2°. Adhesion energy of the metal oxide for oil droplets was investigated also with AFM (Agilent 5500, Agilent). Details of the AFM

probe preparation, experimental setup, and adhesion energy calculation were provided in **Text S6 (SI)**.

Results and Discussion

Fouling tendency of deposited ceramic membranes

Dead-end ultrafiltration with periodical back flush was applied to investigate irreversible fouling of metal oxide-deposited ceramic membranes in the treatment of the emulsion. The deposited membranes have nearly the same pure-water permeability, surface roughness and microstructures as the virgin membrane (**Table S3 and S4, Figure S5 and S6, SI)**. **Figure S7 (SI)** shows the permeate-flux decline of these membranes as a function of filtration duration. The deposited membranes all suffered permeate-flux decline of different extent during filtration, which can be ascribed to membrane fouling and concentration/polarization on the cake layer.[36] Interestingly, two clear stages of the permeate-flux decline were observed before reaching a quasi-steady stage which has a relatively steady permeate flux (**Figure S7, SI and Figure 1**). The initial stage had a relatively slow decline of the permeate flux, being followed by a rapid permeate-flux decline stage. The development of the membrane fouling during the emulsion treatment was hypothesized in **Scheme 1**. At the beginning of the filtration, small oil droplets could directly penetrate and stuck inside membrane pores, which partially blocks the membrane pore leading to a slow decrease of the permeate flux (i.e., the first stage). Meanwhile, some oil droplets also deposit on the membrane surface. Then, the oil droplets would “pile-up” on membrane surface, which promotes the collision and coalescence of oil droplets as the

filtration further proceeds.[37, 38] The membrane pore entrance will consequently be covered by the coalesced oil droplets leading to significant reduction of the effective pore size and a quick decline of the permeate flux (i.e., the second stage). Eventually, a compact oil layer of coalesced droplets spreads out on membrane surface and fully covers on the pore entrance as a "second membrane". [55] This uniform oil layer dominates permeate-flux and oil rejection, and leads to a steady permeate flux (i.e., quasi-steady stage).[39, 40] Since the same O/W emulsion was used, the oil layer formed on each deposited membrane would be similar to each other, which would therefore lead to a similar oil rejection. COD rejection rates of the five deposited membranes (in **Table 1)** further confirmed our hypothesis. 93.2%, 96.1%, and 93.0% of COD rejection (COD = 324 mg O_2/L) were obtained by negatively charged TiO_2-, CeO_2-, and MnO_2- membranes, respectively, while positively charged Fe_2O_3- and CuO-membranes rejected 95.4% and 96.5% COD, respectively. The COD rejection rates of the five metal oxide-deposited membranes were close to each other. In general, solute transmission can be enhanced if the membrane is oppositely charged.[41, 42] The similar COD rejection of these deposited membranes here can be ascribed to a similar and compact oil layer formed on the membrane surface.[39]

Figure 2 presents normalized initial permeate fluxes (NIF_n, n represents the filtration cycles) of the deposited membranes in each cycle of O/W emulsion ultrafiltration. The NIF_n of all the membranes declined as the number of filtration/backwash cycle increased, indicating that hydraulic irreversible membrane fouling increased gradually. In the six filtration cycles, the deposited membranes

suffered different extents of irreversible fouling. Fe_2O_3-membrane showed the best filtration performance and lowest irreversible fouling (NIF_6 = 60%), whereas MnO_2-membrane suffered the most severe fouling (NIF_6 = 34%) of all the membranes. In comparison, TiO_2-, CuO-, and CeO_2- membranes had moderate irreversible fouling (i.e., NIF_6 = 52%, 47%, and 44%, respectively). The irreversible fouling tendency of the deposited membranes follows the order of Fe_2O_3-membrane < TiO_2-membrane < CuO-membrane < CeO_2-membrane < MnO_2-membrane.

Surface properties of the deposition metal oxides

Since the surface roughness and structures are nearly the same, the significant difference in irreversible fouling extent of the deposited membranes is considered to be caused by distinct surface properties of the deposited metal oxides. To elucidate the relationship between metal oxide surface properties and the irreversible fouling tendency, these metal oxides were fully characterized in terms of their surface hydroxyl groups in water, hydrophilicity, surface charge, and adhesion energy for oil droplets.

Surface hydroxyl groups Surface hydroxyl groups of metal oxides (MeO-H) play an important role in influencing their surface properties. Hydroxyl groups can interact with water molecules through chemisorption or hydrogen-bond interactions.[43] In addition, MeO-H formed $Me\text{-}OH_2^+$ or $Me\text{-}O^-$ species through protonation/ deprotonation at pH below or above pH_{pzc} of the metal oxide.[44] The surface hydroxyl groups of the metal oxides can be analyzed with ATR-FTIR.[45-47] The stretching band

of MeO-H can be separated from that of the O-H of bulk water by using D_2O as solvent, where the surface hydroxyl group is deuterated.[45] The surface MeO-D has been reported to have characteristic IR stretching vibration in the range of 2200-2800 cm^{-1}.[43, 46, 48] **Figure 3** shows the ATR-FTIR spectra of the surface MeO-D groups of the metal oxides in D_2O suspensions. The stretching frequencies of MeO-D of MnO_2, CuO, CeO_2, TiO_2, and Fe_2O_3 were 2337, 2339, 2456, 2545, and 2628 cm^{-1}, respectively, indicating that the bond strength of O-D in MeO-D groups of the metal oxides follows the order of $MnO_2 < CuO < CeO_2 < TiO_2 < Fe_2O_3$. A strong O-D bond of the MeO-D group indicates that the metal site (Me) has relatively weak bonding with the O atom of the surface O-D group. The strong O-D bond also implies high electron density of the O-D group and thus possibly high affinity for D_2O molecules through forming strong hydrogen bond. Therefore, the surface hydroxyl groups of Fe_2O_3 probably tend to strongly interact with water molecules through hydrogen bond (i.e. highly hydrophilic), whereas those of MnO_2 and CuO would be significantly less hydrophilic. This hypothesis is confirmed in the following hydrophilicity test.

Hydrophilicity Hydrophilicity is an important parameter for predicting fouling tendency of polymeric membranes: high hydrophilicity usually means low membrane fouling potential in filtration.[49, 50] Metal oxides have been considered to be all hydrophilic. Differences in the hydrophilicity of metal oxides have never been realized until a recent study disclosed that some lanthanide oxides are relatively more hydrophobic than others.[35] The hydrophilicity of the metal oxides used in this study was tested with contact angle measurement. In general, a small contact angle indicates

a high hydrophilicity of the material.[51] Contact angle images of the five metal oxide-deposited wafers taken within 30 s of interaction with water droplets clearly show the differences of their hydrophilicity (**Figure 4a)**. The contact angles of the five metal oxides varied significantly from 26.6º to 71.7º (**Table 1)**. The hydrophilicity of the five metal oxides increases with the order of MnO_2 < CeO_2 < CuO < TiO_2 < Fe_2O_3 (contact angles being 71.7º, 63.6º, 52.8º, 29.8º, 26.6º, respectively). This result supports the infer drawn with the order of IR stretching frequencies of the surface MeO–D bonds of these metal oxides, suggesting that the properties of surface hydroxyl groups largely influence the hydrophilicity of these metal oxides. **Figure 4b** schematically describes how water molecules attach on metal oxides by interaction with surface hydroxyl groups. A monolayer of water molecules interact directly with the surface hydroxyl groups of the metal oxide through hydrogen bonding, and then interact with outer-sphere water molecules also through hydrogen bonding forming multiple layers of water molecules.

Surface charge Surface charge of membrane material influences electrostatic interactions between the membrane and the solutes. Membrane fouling can be enhanced or reduced through electrostatic interactions.[18, 30] As described above, the surface charge of metal oxides is developed through protonation/deprotonation of surface hydroxyl groups, which is pH dependent.[44] At pH 6.0 of the experiments (i.e., the pH of the emulsion), MnO_2, CeO_2, and TiO_2 (pH_{pzc} being 3.8, 4.2, and 3.2, respectively, as shown in **Table 1**) were negatively charged, while Fe_2O_3 and CuO (pH_{pzc} being 6.4 and 9.5, respectively) were positively charged. The surface charge of

metal oxide-deposited membranes was consistent with that of the deposition metal oxides at pH 6.0 (**Figure S8, SI**). Because oil droplets were negatively charged (**Table S1, SI**), electrostatic repulsion between oil droplets and particles of MnO_2, CeO_2, and TiO_2 would occur, while electrostatic attraction would exist between oil droplets and particles of Fe_2O_3 and CuO.

Adhesion energy for oil droplets The absorption fouling of oil on metal oxides is not only influenced by hydrophobic-hydrophilic interactions, hydrogen bonding and electrostatic interactions, but also by van der Waals interactions between metal oxide and oil foulant.[52] AFM is a powerful tool that quantitatively measures the interaction forces/energies at the sub-nano Newton resolution between foulants and metal oxides.[53, 54] To further study the oil fouling potential towards metal oxides, adhesion energy of metal oxides for oil droplets was investigated with AFM. **Figure 5** shows that the least hydrophilic MnO_2 has the highest adhesion energy for oil droplets, whereas the most hydrophilic Fe_2O_3 has the lowest adhesion energy of oil droplets. Adhesion energies of the metal oxides for oil droplets followed the order of Fe_2O_3 < TiO_2 < CeO_2 < CuO < MnO_2. It was noticed also that CuO had higher adhesion energy for oil droplets than CeO_2 while its hydrophilicity was higher. This means that the adhesion between oil droplets and metal oxides is also contributed by electrostatic interaction (CuO is oppositely charged to oil droplets, while CeO_2 is similarly charged to oil droplets).[52] Lower adhesion energy between oil droplets and metal oxide indicates lower oil adsorption tendency on the metal oxide. Accordingly, adsorption fouling of oil on metal oxides would decrease with the decreasing adhesion energy in

order of Fe_2O_3 < TiO_2 < CeO_2 < CuO < MnO_2, which can be inversely correlated to the hydrophilicity of the metal oxides.

Relationship between the surface properties of filtration-layer metal oxide and the irreversible membrane fouling tendency

The irreversible fouling tendency of the five metal oxide-deposited membranes can be correlated very well with surface properties of the metal oxides. The bond strength of surface hydroxyl groups of the metal oxides (MeO–H) largely influences their hydrophilicity, and the hydrophilicity mainly dominates the adsorption fouling of oil on the metal oxides. The hydrophilicity of the metal oxides (MnO_2 < CeO_2 < CuO < TiO_2 < Fe_2O_3) correlates inversely with irreversible fouling tendency of the deposited membranes, and higher hydrophilicity is related to lower irreversible fouling tendency. This result indicates that the hydrophilicity of the filtration-layer metal oxide is a major factor influencing irreversible fouling tendency of ceramic membrane in the O/W emulsion treatment. It is already known that hydrophilic polymeric membrane has low fouling tendency.[55, 56] For ceramic membrane, this is the first time observing the difference of these common metal oxides in hydrophilicity and clearly revealing the dominance of the relative hydrophilicity of filtration-layer metal oxide in membrane fouling tendency.

Surface charge of the metal oxide opposite to that of the emulsion helps to alleviate irreversible membrane fouling in ultrafiltration, which is consistent with our last work regarding the influence of surfactant on ceramic membrane performance in O/W emulsion treatment.[30] The positively charged CuO-membrane suffered less

irreversible fouling than the negatively charged CeO_2-membrane in the treatment of negatively charged emulsion (**Figure 2**), whereas its adsorption energy for oil was higher than that of CeO_2 (**Figure 5**). Irreversible membrane fouling is caused by 1) pore blockage by tiny oil droplets and 2) strong adsorption of oil droplets on membrane surface and pores.[20] Although the CuO-membrane has more adsorption fouling than the CeO_2-membrane, it may have less pore blockage fouling and thus overall less irreversible fouling. Cross-section SEM images of the virgin and the fouled CuO- and CeO_2- membranes support this hypothesis (**Figure S9, SI)**. The oxide particles in the filtration layer of CuO- and CeO_2- membranes (**Figure S9b and S9c, SI**) showed larger sizes than that of the virgin membrane (**Figure S9a, SI**). This indicates that oil droplets penetrated into membrane pores and covered on the oxide particles during filtration. The oxide particle size of the CuO-membrane was smaller than that of CeO_2-membrane (**Figure S9b and S9c, SI**), indicating less oil droplet penetration into the CuO-membrane pores and covering on the oxide particles. Less pore blockage fouling of positively charged CuO-membrane could probably be ascribed to 1) the adsorption of some negatively charged surfactant-SDBS molecules on membrane surface and pores, which prevent the penetration of some oil droplets into the pores (i.e., surfactant barrier),[42] and 2) the subsequent coalescence of oil droplets near membrane surface because of the less stabilization SDBS for oil droplets (i.e., demulsification), which leads to more large oil droplets easily rejected on membrane surface and less small oil droplets available to penetrate into membrane pores (**Scheme S1, SI**).

366 It should be noticed that although the CuO-membrane oppositely charged to oil
367 droplets may suffer less irreversible fouling caused by pore blockage, it still has
368 overall more irreversible fouling than the TiO_2-membrane similarly charged to oil
369 droplets. This is probably because the CuO-membrane suffered much more
370 irreversible adsorption fouling than the more hydrophilic TiO_2-membrane (according
371 to the adhesion energy shown in **Figure 5**). This fact again confirms that the
372 hydrophilicity is a more significant factor influencing the irreversible fouling
373 tendency of the ceramic membrane in O/W emulsion treatment.

374 **Environmental significance:**

375 Ceramic membrane ultrafiltration is an ideal treatment process for O/W emulsions
376 daily produced in many industrial activities. Severe irreversible membrane fouling
377 compromises the performance of ceramic membrane in O/W emulsion treatment,
378 where filtration-layer material plays a crucial role. The filtration-layer material of low
379 fouling tendency is highly desirable for sustainable O/W emulsion treatment. This
380 study clearly shows the relationship between the surface properties of the
381 filtration-layer metal oxides and the membrane fouling tendency, which provides a
382 theoretical foundation to guide the selection/preparation/modification of ceramic
383 membranes for sustainable O/W emulsion treatment. In addition, the result suggests
384 that highly hydrophilic metal oxides (e.g., Fe_2O_3) can be potential filtration-layer
385 materials of the ceramic membrane for O/W emulsion treatment.

386 **ASSOCIATED CONTENT**

387 **Supporting Information.**

Six texts, four tables, ten figures and one scheme are included in the supporting information. This information is available free of charge via the Internet at http://pubs.acs.org/

AUTHOR INFORMATION

Corresponding Author

*Tel: +86 451 86283010. Fax: +86 451 86283010. E-mail: majun@hit.edu.cn (J.M.)

*Tel: +61 89266 9793. E-mail: jean-philippe.croue@curtin.edu.au (J.P. Croué).

ACKNOWLEDGEMENTS

This work was supported by and conducted at King Abdullah University of Science and Technology (KAUST). Part of the research is also support by Natural Science Foundation of China (No.51378141). The authors want to thank Saudi Aramco for providing the crude oil for the experiment, Dr. Yingbang Yao of Thin Film Lab of KAUST for his help in PLD deposition, Ms. Nini Wei of Advanced Nanofabrication Imaging and Characterization Lab of KAUST for her help in FIB and STEM, and Dr. Cyril Aubry of WDRC of KAUST for AFM test.

Literature Cited

1. Marchese, J.; Ochoa, N. A.; Pagliero, C.; Almandoz, C., Pilot-Scale Ultrafiltration of an Emulsified Oil Wastewater. *Environ. Sci. Technol.* **2000,** *34*, (14), 2990-2996.
2. Križan Milić, J.; Murić, A.; Petrinić, I.; Simonič, M., Recent Developments in Membrane Treatment of Spent Cutting-Oils: A Review. *Ind. Eng. Chem. Res.* **2013,** *52*, (23), 7603-7616.
3. Kong, J.; Li, K., Oil removal from oil-in-water emulsions using PVDF membranes. *Sep. Purif. Technol.* **1999,** *16*, (1), 83-93.
4. Bevis, A., The treatment of oily water by coalescing. *Filtr. Sep.* **1992,** *29*, (4), 295-300.
5. Baker, R. W., Research needs in the membrane separation industry: Looking back, looking forward. *J. Membr. Sci.* **2010,** *362*, (1-2), 134-136.
6. Bensadok, K.; Belkacem, M.; Nezzal, G., Treatment of cutting oil/water emulsion by coupling

coagulation and dissolved air flotation. *Desalination* **2007,** *206*, (1-3), 440-448.
7. Song, Y. C.; Kim, I. S.; Koh, S. C., Demulsification of oily wastewater through a synergistic effect of ozone and salt. *Water Sci. Technol.* **1998,** *38*, (4-5), 247-253.
8. Daiminger, U.; Nitsch, W.; Plucinski, P.; Hoffmann, S., Novel techniques for iol/water separation. *J. Membr. Sci.* **1995,** *99*, (2), 197-203.
9. Hong, A.; Fane, A. G.; Burford, R., Factors affecting membrane coalescence of stable oil-in-water emulsions. *J. Membr. Sci.* **2003,** *222*, (1–2), 19-39.
10. Chen, W.; Peng, J.; Su, Y.; Zheng, L.; Wang, L.; Jiang, Z., Separation of oil/water emulsion using Pluronic F127 modified polyethersulfone ultrafiltration membranes. *Sep. Purif. Technol.* **2009,** *66*, (3), 591-597.
11. Zhao, X.; Su, Y.; Chen, W.; Peng, J.; Jiang, Z., Grafting perfluoroalkyl groups onto polyacrylonitrile membrane surface for improved fouling release property. *J. Membr. Sci.* **2012,** *415-416*, 824-834.
12. Li, L.; Ding, L.; Tu, Z.; Wan, Y.; Clausse, D.; Lanoisellé, J.-L., Recovery of linseed oil dispersed within an oil-in-water emulsion using hydrophilic membrane by rotating disk filtration system. *J. Membr. Sci.* **2009,** *342*, (1-2), 70-79.
13. Zhang, W. B.; Zhu, Y. Z.; Liu, X.; Wang, D.; Li, J. Y.; Jiang, L.; Jin, J., Salt-Induced Fabrication of Superhydrophilic and Underwater Superoleophobic PAA-g-PVDF Membranes for Effective Separation of Oil-in-Water Emulsions. *Angew.Chem.Int. Ed.* **2014,** *53*, (3), 856-860.
14. Yang, Y.; Wang, H.; Li, J.; He, B.; Wang, T.; Liao, S., Novel functionalized nano-TiO2 loading electrocatalytic membrane for oily wastewater treatment. *Environ. Sci. Technol.* **2012,** *46*, (12), 6815-21.
15. Deriszadeh, A.; Husein, M. M.; Harding, T. G., Produced Water Treatment by Micellar-Enhanced Ultrafiltration. *Environ. Sci. Technol* **2010,** *44*, (5), 1767-1772.
16. Gourgouillon, D.; Schrive, L.; Sarrade, S., An Environmentally Friendly Process for the Regeneration of Used Oils. *Environ. Sci. Technol* **2000,** *34*, (16), 3469-3473.
17. Chen, W.; Su, Y.; Zheng, L.; Wang, L.; Jiang, Z., The improved oil/water separation performance of cellulose acetate-graft-polyacrylonitrile membranes. *J. Membr. Sci.* **2009,** *337*, (1-2), 98-105.
18. Lobo, A.; Cambiella, Á.; Benito, J. M.; Pazos, C.; Coca, J., Ultrafiltration of oil-in-water emulsions with ceramic membranes: Influence of pH and crossflow velocity. *J. Membr. Sci.* **2006,** *278*, (1-2), 328-334.
19. Karhu, M.; Kuokkanen, T.; Ramo, J.; Mikola, M.; Tanskanen, J., Performance of a commercial industrial-scale UF-based process for treatment of oily wastewaters. *J. Environ.Manage.* **2013,** *128*, 413-20.
20. Zhou, J. E.; Chang, Q. B.; Wang, Y. Q.; Wang, J. M.; Meng, G. Y., Separation of stable oil-water emulsion by the hydrophilic nano-sized ZrO2 modified Al2O3 microfiltration membrane. *Sep. Purif. Technol.* **2010,** *75*, (3), 243-248.
21. Costa, A. R.; de Pinho, M. N., Effect of membrane pore size and solution chemistry on the ultrafiltration of humic substances solutions. *J. Membr. Sci.* **2005,** *255*, (1–2), 49-56.
22. Wen, Q.; Di, J.; Jiang, L.; Yu, J.; Xu, R., Zeolite-coated mesh film for efficient oil–water separation. *Chem. Sci.* **2013,** *4*, (2), 591.
23. Karimnezhad, H.; Rajabi, L.; Salehi, E.; Derakhshan, A. A.; Azimi, S., Novel nanocomposite Kevlar fabric membranes: Fabrication characterization, and performance in oil/water separation. *Appl. Surf. Sci.* **2014,** *293*, 275-286.
24. Mansourizadeh, A.; Azad, A. J., Preparation of blend polyethersulfone/cellulose

459 acetate/polyethylene glycol asymmetric membranes for oil-water separation. *J. Polym. Res.* **2014,** *21*, (3),
460 9.
461 25. Komolikov, Y. I.; Blaginina, L. A., Technology of Ceramic Micro and Ultrafiltration Membranes
462 (Review). *Refract. Ind. Ceram.* **2002,** *43*, (5-6), 181-187.
463 26. Benfer, S.; Árki, P.; Tomandl, G., Ceramic Membranes for Filtration Applications — Preparation
464 and Characterization. *Adv. Eng. Mater.* **2004,** *6*, (7), 495-500.
465 27. Lee, D. W.; Yoo, B. R., Advanced metal oxide (supported) catalysts: Synthesis and applications.
466 *J. Ind. and Eng. Chem.* **2014,** *20*, (6), 3947-3959.
467 28. Wachs, I. E., Recent conceptual advances in the catalysis science of mixed metal oxide catalytic
468 materials. *Cheminform* **2005,** *100*, (s 1–2), 79-94.
469 29. Wu, W.; Huang, Z.-H.; Lim, T.-T., Recent development of mixed metal oxide anodes for
470 electrochemical oxidation of organic pollutants in water. *Appl. Catal. A: Gen.* **2014,** *480*, 58-78.
471 30. Lu, D.; Zhang, T.; Ma, J., Ceramic Membrane Fouling during Ultrafiltration of Oil/Water
472 Emulsions: Roles Played by Stabilization Surfactants of Oil Droplets. *Environ. Sci. Technol.* **2015,** *49*,
473 (7), 4235-44.
474 31. Fowler, S. D.; Greenspan, P., Application of Nile red, a fluorescent hydrophobic probe, for the
475 detection of neutral lipid deposits in tissue sections: comparison with oil red O. *J. Histochem. Cytochem.*
476 **1985,** *33*, (8), 833-6.
477 32. Quéré, D., Wetting and Roughness. *Annu. Rev. Mater. Res.* **2008,** *38*, (1), 71-99.
478 33. Yoshimitsu, Z.; Nakajima, A.; Watanabe, T.; Hashimoto, K., Effects of Surface Structure on the
479 Hydrophobicity and Sliding Behavior of Water Droplets. *Langmuir* **2002,** *18*, (15), 5818-5822.
480 34. Eral, H. B.; 't Mannetje, D. J. C. M.; Oh, J. M., Contact angle hysteresis: a review of fundamentals
481 and applications. *Colloid Polym. Sci.***2013,** *291*, (2), 247-260.
482 35. Azimi, G.; Dhiman, R.; Kwon, H. M.; Paxson, A. T.; Varanasi, K. K., Hydrophobicity of rare-earth
483 oxide ceramics. *Nat. Mater.* **2013,** *12*, (4), 315-20.
484 36. Meng, F.; Liao, B.; Liang, S.; Yang, F.; Zhang, H.; Song, L., Morphological visualization,
485 componential characterization and microbiological identification of membrane fouling in membrane
486 bioreactors (MBRs). *J. Membr. Sci.* **2010,** *361*, (1-2), 1-14.
487 37. Zhao, F.; Clarens, A.; Skerlos, S. J., Optimization of metalworking fluid microemulsion surfactant
488 concentrations for microfiltration recycling. *Environ. Sci. Technol.* **2007,** *41*, (3), 1016-23.
489 38. Zhao, F.; Urbance, M.; Skerlos, S. J., Mechanistic Model of Coaxial Microfiltration for
490 Semi-Synthetic Metalworking Fluid Microemulsions. *J. Manuf. Sci. Eng.* **2004,** *126*, (3), 435-444.
491 39. Cumming, I. W.; Holdich, R. G.; Smith, I. D., The rejection of oil using an asymmetric metal
492 microfilter to separate an oil in water dispersion. *Water Res.* **1999,** *33*, (17), 3587-3594.
493 40. Yazdanshenas, M.; Soltanieh, M.; Tabatabaei Nejad, S. A. R.; Fillaudeau, L., Cross-flow
494 microfiltration of rough non-alcoholic beer and diluted malt extract with tubular ceramic membranes:
495 Investigation of fouling mechanisms. *J. Membr. Sci.* **2010,** *362*, (1-2), 306-316.
496 41. Burns, D. B.; Zydney, A. L., Contributions to electrostatic interactions on protein transport in
497 membrane systems. *Aiche J.* **2001,** *47*, (5), 1101-1114.
498 42. Peeva, P. D.; Knoche, T.; Pieper, T.; Ulbricht, M., Performance of Thin-Layer Hydrogel
499 Polyethersulfone Composite Membranes during Dead-End Ultrafiltration of Various Protein Solutions.
500 *Ind. Eng. Chem. Res.* **2012,** *51*, (21), 7231-7241.
501 43. Takeuchi, M.; Martra, G.; Coluccia, S.; Anpo, M., Investigations of the structure of H2O clusters
502 adsorbed on TiO2 surfaces by near-infrared absorption spectroscopy. *J. Phys. Chem. B* **2005,** *109*, (15),

503 7387-91.
504 44. Hohl, H.; Sigg, L.; Stumm, W., Characterization of surface chemical properties of oxides in natural
505 waters. *Adv. Chem. Ser.* **1980,** *189*, 1-31.
506 45. Tejedor-Tejedor, M. I.; Anderson, M. A., "In situ" ATR-Fourier transform infrared studies of the
507 goethite (α-FeOOH)-aqueous solution interface. *Langmuir* **1986,** *2*, (2), 203-210.
508 46. Zhang, T.; Li, C.; Ma, J.; Tian, H.; Qiang, Z., Surface hydroxyl groups of synthetic α-FeOOH in
509 promoting OH generation from aqueous ozone: Property and activity relationship. *Appl. Catal., B:*
510 *Environ.* **2008,** *82*, (1-2), 131-137.
511 47. Tejedor-Tejedor, M. I.; Anderson, M. A., The protonation of phosphate on the surface of goethite as
512 studied by CIR-FTIR and electrophoretic mobility. *Langmuir* **1990,** *6*, (3), 602-611.
513 48. Yalamanchili, M. R.; Atia, A. A.; Miller, J. D., Analysis of interfacial water at a hydrophilic silicon
514 surface by in-situ FTIR/internal reflection spectroscopy. *Langmuir* **1996,** *12*, (17), 4176-4184.
515 49. Jung, Y. C.; Bhushan, B., Wetting Behavior of Water and Oil Droplets in Three-Phase Interfaces for
516 Hydrophobicity/philicity and Oleophobicity/philicity†. *Langmuir* **2009,** *25*, (24), 14165-14173.
517 50. Zhao, X.; Chen, W.; Su, Y.; Zhu, W.; Peng, J.; Jiang, Z.; Kong, L.; Li, Y.; Liu, J., Hierarchically
518 engineered membrane surfaces with superior antifouling and self-cleaning properties. *J. Membr. Sci.*
519 **2013,** *441*, (0), 93-101.
520 51. Shao, L.; Wang, Z. X.; Zhang, Y. L.; Jiang, Z. X.; Liu, Y. Y., A facile strategy to enhance PVDF
521 ultrafiltration membrane performance via self-polymerized polydopamine followed by hydrolysis of
522 ammonium fluotitanate. *J. Membr. Sci.* **2014,** *461*, (0), 10-21.
523 52. Butt, H.-J.; Cappella, B.; Kappl, M., Force measurements with the atomic force microscope:
524 Technique, interpretation and applications. *Surf. Sci.Rep.* **2005,** *59*, (1-6), 1-152.
525 53. Li, Q.; Elimelech, M., Organic Fouling and Chemical Cleaning of Nanofiltration Membranes:
526 Measurements and Mechanisms. *Environ. Sci. Technol.* **2004,** *38*, (17), 4683-4693.
527 54. Wang, L.; Miao, R.; Wang, X.; Lv, Y.; Meng, X.; Yang, Y.; Huang, D.; Feng, L.; Liu, Z.; Ju, K.,
528 Fouling behavior of typical organic foulants in polyvinylidene fluoride ultrafiltration membranes:
529 characterization from microforces. *Environ. Sci. Technol.* **2013,** *47*, (8), 3708-14.
530 55. Adout, A.; Kang, S.; Asatekin, A.; Mayes, A. M.; Elimelech, M., Ultrafiltration Membranes
531 Incorporating Amphiphilic Comb Copolymer Additives Prevent Irreversible Adhesion of Bacteria.
532 *Environ. Sci. Technol.* **2010,** *44*, (7), 2406-2411.
533 56. Kang, S.; Asatekin, A.; Mayes, A. M.; Elimelech, M., Protein antifouling mechanisms of PAN UF
534 membranes incorporating PAN-g-PEO additive. *J. Membr. Sci.* **2007,** *296*, (1–2), 42-50.
535
536
537
538
539
540
541
542
543

Table 1. Surface properties of the metal oxides and COD rejection rates of ceramic membranes deposited with these metal oxides for the O/W emulsion

Metal oxide	Contact angle (degrees)	pH_{pzc}	Surface charge [a]	COD rejection %
Fe_2O_3	26.6 ± 1.6	6.4	+	95.4
CuO	52.8 ± 1.6	9.5	+	93.2
TiO_2	29.8 ± 1.5	3.2	-	96.5
CeO_2	63.6 ± 1.9	4.2	-	96.1
MnO_2	71.7 ± 1.1	3.8	-	93.0

[a] Surface charge of metal oxides under experimental filtration conditions (pH = 6.0).

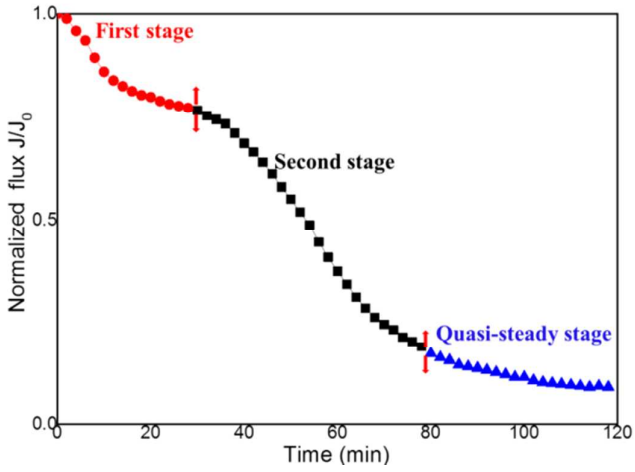

Figure 1. Normalized permeate-flux decline of Fe_2O_3-membrane for O/W emulsion treatment in a long run without back flush

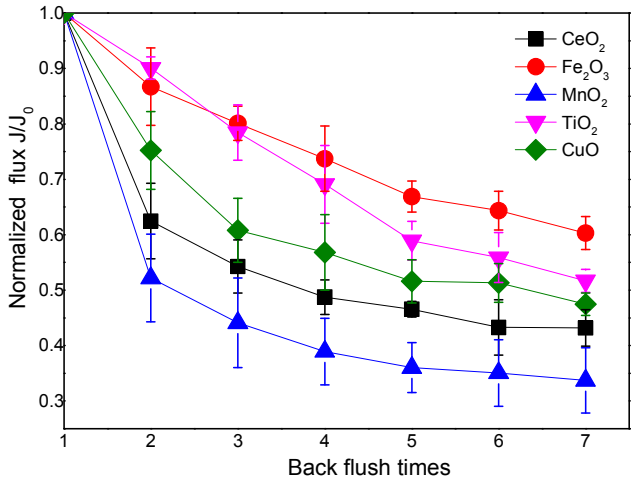

Figure 2. Decline of normalized initial permeate-flux of ceramic membranes deposited with different metal oxides in seven cycles of O/W emulsion filtration.

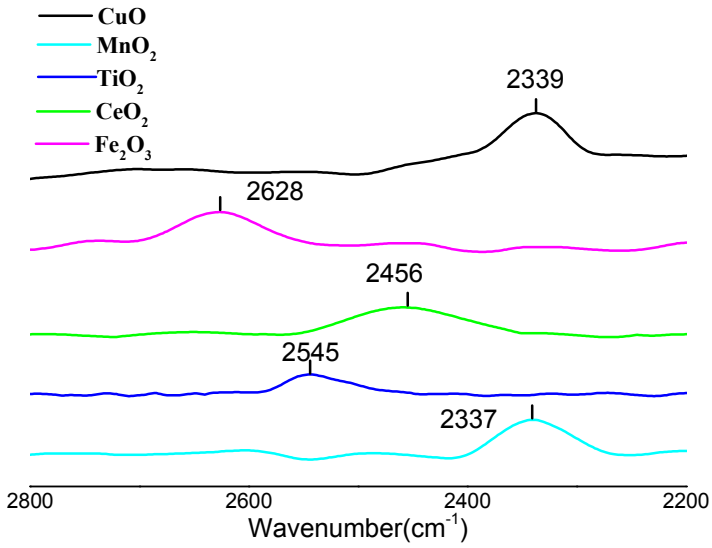

Figure 3. ATR-FTIR spectra of surface MeO-D groups of metal oxides immersed in D_2O (pD = 6.0).

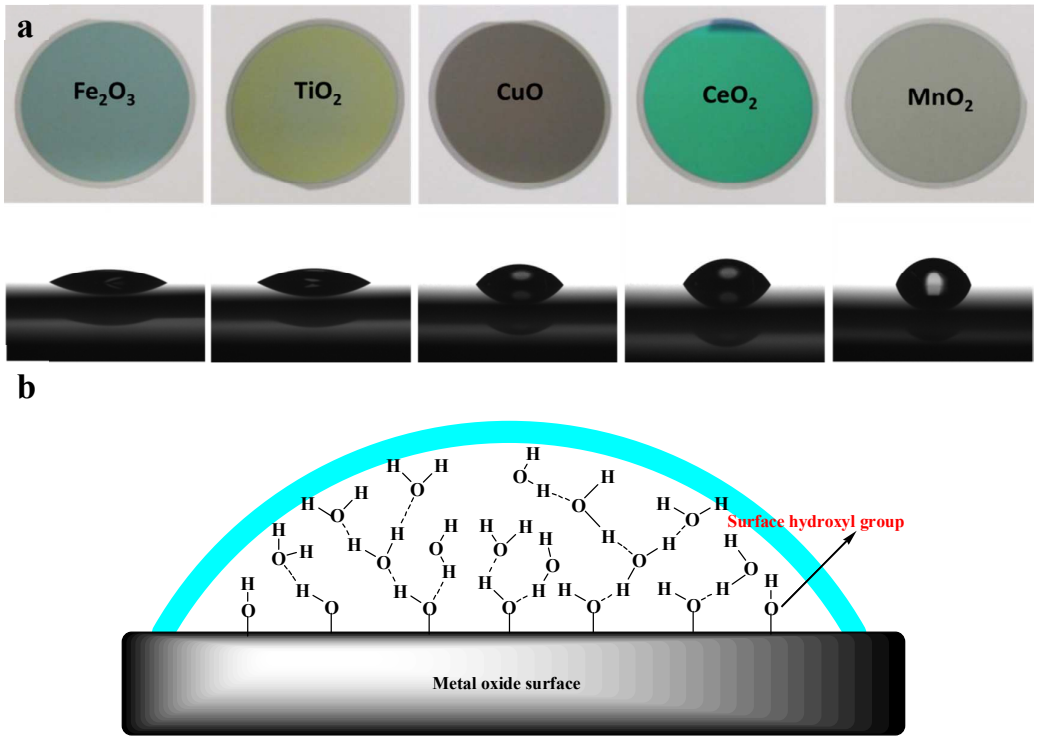

Figure 4. Optical images and contact angle images of metal oxides deposited on silicon wafers (a). A scheme of interaction between water droplet and metal oxide surface (b).

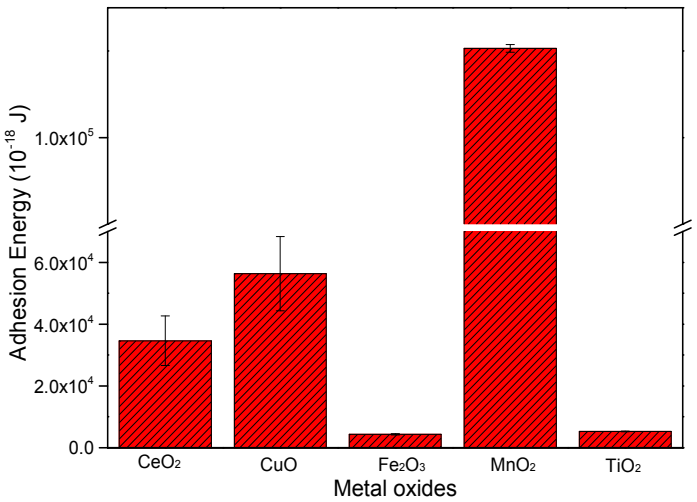

Figure 5. Adhesion energy between metal oxides and oil droplets.

589

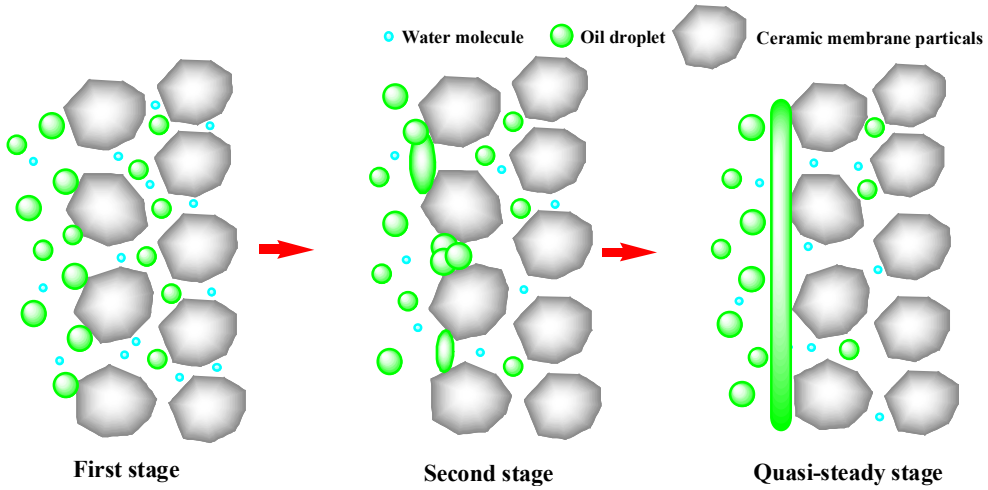

590

591 Scheme 1. Possible membrane fouling stages of ceramic membrane during O/W emulsion treatment.

592

593

594

595